A European aerosol phenomenology -4: Harmonized concentrations of carbonaceous aerosol at 10 regional background sites across Europe

F. Cavalli, A. Alastuey, H. Areskoug, D. Ceburnis, J. Čech, J. Genberg, R. M. Harrison, J. L. Jaffrezo, G. Kiss, P. Laj, et al.

Atmospheric Environment 144 (2016) 133–145

Contents lists available at ScienceDirect

Atmospheric Environment

journal homepage: www.elsevier.com/locate/atmosenv

A European aerosol phenomenology -4: Harmonized concentrations of carbonaceous aerosol at 10 regional background sites across Europe

F. Cavalli [a], A. Alastuey [b], H. Areskoug [c], D. Ceburnis [d], J. Čech [e], J. Genberg [f], R.M. Harrison [g, h], J.L. Jaffrezo [i], G. Kiss [j], P. Laj [i, k], N. Mihalopoulos [l, m], N. Perez [b], P. Quincey [n], J. Schwarz [o], K. Sellegri [p], G. Spindler [q], E. Swietlicki [f], C. Theodosi [m], K.E. Yttri [r], W. Aas [r], J.P. Putaud [a, *]

[a] European Commission, Joint Research Centre (JRC), Directorate for Energy, Transport and Climate, Air and Climate Unit, Via E. Fermi 2749, I-21027, Ispra, VA, Italy
[b] Instituto de Diagnostico Ambiental y Estudios Del Agua, Consejo Superior de Investigaciones Cientificas, C/ Jordi Girona 18-26, 08034, Barcelona, Spain
[c] Stockholm University, ACES, SE-106 91, Stockholm, Sweden
[d] School of Physics and Centre for Climate & Air Pollution Studies, Ryan Institute, National University of Ireland Galway, University Road, Galway, Ireland
[e] Czech Hydrometeorological Institute, Na Šabatce 2050/17, CZE-143 06, Praha 412-Komořany, Czech Republic
[f] Lund University, Department of Physics, Division of Nuclear Physics, S-221 00, Lund, Sweden
[g] Division of Environmental Health and Risk Management, School of Geography, Earth and Environmental Sciences, University of Birmingham, Edgbaston, Birmingham, B15 2TT, United Kingdom
[h] Department of Environmental Sciences / Center of Excellence in Environmental Studies, King Abdulaziz University, PO Box 80203, Jeddah, 21589, Saudi Arabia
[i] Université Grenoble-Alpes / CNRS, Laboratoire de Glaciologie et Géophysique de l'Environnement, Rue Molière, F-38402, Saint Martin D'Hères Cedex, France
[j] MTA-PE Air Chemistry Research Group, Egyetem 10, 8200, Veszprém, Hungary
[k] Department of Physics, University of Helsinki, P.O. Box 64, FIN-00014, Helsinki, Finland
[l] Institute for Environmental Research & Sustainable Development, National Observatory of Athens, I. Metaxa & Vas. Pavlou, GR-15236, Palea Penteli, Greece
[m] University of Crete, Chemistry Department, 71003, Heraklion, Crete, Greece
[n] Environment Division, National Physical Laboratory, Teddington, TW11 0LW, UK
[o] Institute of Chemical Process Fundamentals CAS, 16502, Prague 6, Czech Republic
[p] Laboratoire de Météorologie Physique LaMP-CNRS/OPGC, Université Blaise Pascal, 24 Avenue des Landais, F-63170, Aubière, France
[q] Leibniz Institute for Tropospheric Research, Permoserstraße 15, 04318, Leipzig, Germany
[r] NILU – Norwegian Institute for Air Research, P.O. Box 100, N-2027, Kjeller, Norway

HIGHLIGHTS

- Artefacts bias the sampling of carbonaceous matter by quartz fibre filters.
- Identical thermal protocols run on various instruments produce different results.
- Seasonal variations can be observed in intensive carbonaceous aerosol variables.
- TC/PM_{10} ratios range from 12 to 34% across European regional background sites.
- Site-mean EC/TC ratios range from 10 to 22% and get similar at all sites in winter.

ARTICLE INFO

Article history:
Received 1 April 2016
Received in revised form
21 July 2016
Accepted 25 July 2016
Available online 28 August 2016

Keywords:
Aerosol

ABSTRACT

Although particulate organic and elemental carbon (OC and EC) are important constituents of the suspended atmospheric particulate matter (PM), measurements of OC and EC are much less common and more uncertain than measurements of e.g. the ionic components of PM. In the framework of atmospheric research infrastructures supported by the European Union, actions have been undertaken to determine and mitigate sampling artefacts, and assess the comparability of OC and EC data obtained in a network of 10 atmospheric observatories across Europe. Positive sampling artefacts (from 0.4 to 2.8 μg C/m^3) and analytical discrepancies (between −50% and +40% for the EC/TC ratio) have been taken into account to generate a robust data set, from which we established the phenomenology of carbonaceous aerosols at

* Corresponding author.
E-mail address: jean.putaud@jrc.ec.europa.eu (J.P. Putaud).

http://dx.doi.org/10.1016/j.atmosenv.2016.07.050

Carbonaceous
PM
Phenomenology
Europe

regional background sites in Europe. Across the network, TC and EC annual average concentrations range from 0.4 to 9 μg C/m^3, and from 0.1 to 2 μg C/m^3, respectively. TC/PM_{10} annual mean ratios range from 0.11 at a Mediterranean site to 0.34 at the most polluted continental site, and TC/$PM_{2.5}$ ratios are slightly greater at all sites (0.15–0.42). EC/TC annual mean ratios range from 0.10 to 0.22, and do not depend much on PM concentration levels, especially in winter. Seasonal variations in PM and TC concentrations, and in TC/PM and EC/TC ratios, differ across the network, which can be explained by seasonal changes in PM source contributions at some sites.

1. Introduction

Carbonaceous aerosol is a complex mixture of many organics (the OC fraction) and elemental carbon (EC). As some of these organics are highly toxic and elemental carbon is present largely as solid insoluble nanoparticles, carbonaceous aerosol could have a larger health impact than other PM constituents (Cassee et al., 2013; WHO, 2013). Carbonaceous particles also play a clear role in climate change through direct and indirect radiative forcing, although the magnitude of these effects is still quite uncertain (Boucher et al., 2013). During the last decade, OC and EC data have been measured at many sites across Europe, (e.g. Pio et al., 2007; Yttri et al., 2007a; Querol et al., 2013). Such measurements are extremely valuable for assessing temporal trends and spatial variability in OC and EC concentrations (Yttri et al., 2007b; Putaud et al., 2010; Tørseth et al., 2012). In-situ measurements in general are also essential for calibrating or validating data retrievals from remote sensing and model outputs. However, the accuracy and precision of particulate OC and EC data is particularly questionable since various factors can lead to large errors in OC and EC data, both at the sampling and analysis stages.

Artefacts can affect the sampling of particulate organic carbon, which is always carried out on quartz fibre filters. They have been extensively studied in the USA for more than 2 decades (e.g. McDow and Huntzicker, 1990; Turpin and Huntzicker, 1994; Mader et al., 2001; Watson et al., 2009). They found positive sampling artefacts ranging between 0.2 and 3 μgC/m^3, increasing with the particulate total carbon (TC) concentration, and decreasing with the sampling face velocity. In Europe, less information is available. From studies by Viana et al. (2006) and Schwarz et al. (2008), it could be estimated that the contribution of positive artefacts to the total amount of OC collected by a quartz fibre filter was on average about 30% in Ghent (Belgium), and Prague, (Czech Republic). At Nordic sites for 1 week sampling times, the mean positive sampling artefact ranged from 11% to 18% of OC (Yttri et al., 2011a).

Analytically, atmospheric particulate carbon has traditionally been split into OC and EC, although drawing a clear border between organic macro-molecules (OC) and small clusters of (possibly amorphous) EC is challenging (Baumgardner et al., 2012). Furthermore, charring can transform a part of OC into species looking like EC during the analysis, which must be accounted for (Chow et al., 1993; Birch and Cary, 1996). Eventually, OC and EC are operationally defined, and values produced by various laboratories using identical or different methods can be very different from each other, especially for EC. Various studies report differences up to a factor of 2 when comparing EC resulting from different methods, and reproducibility standard deviations in the range of 10–25% for the determination of EC by a given method (e.g. Watson et al., 2005; Karanasiou et al., 2015).

The current study reports on a specific action aimed at providing robust and comparable data on particulate carbonaceous aerosol across Europe. This long-term action was carried out under the European Research Infrastructure projects EUSAAR (European Supersites for Atmospheric Aerosol Research) and ACTRIS (Aerosols, Clouds, and trace gases Research Infrastructure, www.actris.eu). Coordinated experiments were performed to assess the positive and negative artefacts which affect particulate OC sampling during different seasons at several regional background sites across Europe. A sampling train (Fig. S1), which minimizes positive sampling artefacts without significantly increasing negative artefacts was also tested and validated. The comparability of the analyses performed by all the laboratories which produced the data discussed in the current study was also assessed on the basis of annual inter-laboratory comparisons.

Combining our knowledge of site-dependent sampling artefacts and laboratory-dependent possible analytical discrepancies allowed us to construct the most robust data set on particulate carbonaceous aerosol available for Europe so far. We can thus discuss with a level of confidence previously not available the similarities and differences in carbonaceous aerosol concentration, its contribution to PM mass, and its composition in terms of OC and EC, among 10 regional background sites across Europe. Seasonal variations are also examined, which can provide information on carbonaceous aerosol sources at some of these sites.

2. Experimental

The data we discuss here were obtained between 2008 and 2011 as a result of the collaboration among research institutes running 10 atmospheric observatories at regional background sites located across Europe (Fig. 1): Aspvreten (APT), Birkenes (BIR), Vavihil (VAV), Harwell (HRL), Melpitz (MEL), Kosetice (KOS), Ispra (IPR), Puy de Dôme (PUY), Montseny (MSY), and Finokalia (FIK). Specific experiments related to sampling artefacts were also performed at Hurdal (HUR), Mace Head (MHD), and K-puszta (KPS).

2.1. Mass and carbonaceous aerosol concentration measurements

2.1.1. Sampling

Sampling was performed using quartz fibre filters of different types for periods between 24 and 168 h at face velocities ranging 20–53 cm/s (Table 1). Denuders (P/Nr 55-008923-002, Air Monitors, UK) were continuously used for daily measurements for at least one size fraction at APT, VAV, and IPR, as well as in KOS from Sep. 2011. Quartz fibre back up filters were used for daily measurements at KOS, and at 7 more sites to assess positive sampling artefacts during specific experiments (Table 1). At the remaining 4 sites, bare quartz fibre filters only were used.

2.1.2. Analysis

PM_{10} and $PM_{2.5}$ mass concentrations were determined by gravimetric analyses of the quartz fibre filters used for OC and EC measurements at 4 sites, by gravimetric analyses of Teflon™ and Emfab™ filters collected simultaneously at KOS and HRL,

Fig. 1. Observatories from which data are presented. Sites in italics were used for studying sampling artefacts only. Photo: http://www.esa.int/spaceinimages/Images/2003/09/A_mosaic_of_satellite_images_showing_a_cloud-free_Europe.

respectively, and by independent on-line methods at APT, VAV and FIK (Table 1). No correction was applied to PM_{10} and $PM_{2.5}$ mass to account for possible discrepancies between various measurement methods. No PM data were available from PUY.

Thermal-optical analysers with a charring correction based on filter transmittance monitoring were used to produce all the OC and EC data sets discussed here except one (Table 1). Among those, all instruments but one (Table 1) ran the thermal protocol EUSAAR-2 (Cavalli et al., 2010).

2.2. Sampling artefacts

2.2.1. Positive sampling artefact assessment

To assess the magnitude of the positive sampling artefact, back up filter methods known as the quartz behind Teflon™ (QbT) and the quartz behind quartz (QbQ) techniques (see the supplementary material for details) were implemented for different seasons at HUR, VAV, MHD, KOS, KPS, IPR, and PUY, HUR, VAV, MSY, KOS, respectively (Table 1). Further details are provided in the supplementary material.

Measurements performed at these 8 sites across Europe showed seasonal (Wi, Sp, Su, Au) mean positive sampling artefacts ranging from 0.4 to 2.8 μgC/m^3 (Fig. 2). These positive artefacts accounted on average for 14–70% of the amount of TC simultaneously collected by a bare front quartz fibre filter at these sites (Fig. 2). Positive sampling artefacts are thus significant in all areas of Europe and for all seasons. It should be noticed that the site where the contribution of positive artefacts was highest (HUR) is one of the two sites where its absolute value was the lowest. This illustrates that positive sampling artefacts can also be relevant at the least polluted sites.

2.2.2. Negative sampling artefact determination

Negative sampling artefacts were estimated at IPR by measuring the amount of OC collected on back-up filters with the EUSAAR sampling train made of a denuder, and a series of 3 fibre filters (Fig. S1). Without correcting the data for the denuder breakthrough, the magnitude of the negative artefacts represented 5 ± 2% of the amount of C collected by the front quartz fibre filter (24hr sampling from 08:00 to 08:00 UTC, 20 cm s^{-1} face velocity, 1 h average temperature ranging from −5 to +21 °C), with no dependence on ambient temperature. This confirms the results obtained at several sites in the USA (e.g. Subramanian et al., 2004; Watson et al., 2009) showing that negative sampling artefacts are generally small compared to positive artefacts.

2.2.3. Impacts of the denuder use

The suitability for the continuous monitoring of particulate OC and EC of the C-monolith denuders recently made commercially available (Air Monitors, UK) was tested at various sites across Europe as part of EUSAAR. A detailed description of the EUSAAR denuder validation tests is reported in the supplementary material.

In short, laboratory tests demonstrated that particle losses in the EUSAAR denuder (see Fig. S1) are acceptable, i.e. <3% (Fig. S3), and field experiments showed that positive artefacts are reduced to <0.1–0.5 μgC/m^3 (seasonal average), representing 1–18%

Table 1
Location and experimental conditions at the sites providing data for this work. Sites in italics provided data related to sampling artefact assessment only.

		Location			Sampling						Analyses	
		Latitude	Longitude	Altitude	Face velocity (cm/s)	Duration (hrs)	Filter type	Denuder	QbQ	QbT	Mass	Carbon
PUY	Puy de Dôme	45°46′N	2°57′E	1465	36	24	Whatman QMA	C	C			EUSAAR-2
BIR	Birkenes	58°23′N	8°15′E	190	46	168	Whatman QMA				grav.	EUSAAR-2
HUR	*Hurdal*	*60°22′N*	*11°05′E*	*300*	46	*24*	*Whatman QMA*	*C*	*C*	*C*	*N/A*	EUSAAR-2
APT	Aspvreten	58°48′N	17°23′E	20	46	24	Munktell T293	Y			TEOM	EUSAAR-2
MHD	*Mace Head*	*53°10′N*	*9°30′W*	*15*	*20*	*24*	*PALL-2500QAT*	*C*		*C*	*N/A*	EUSAAR-2
HRL	Harwell	51°34′N	1°19′W	137	46	24	PALL-2500QAT				grav.	NIOSH-like
VAV	Vavihill	56°01′N	13°09′E	175	46	72	PALL-2500QAT	Y	C	C	TEOM	EUSAAR-2
MSY	Montseny	41°46′N	2°21′E	700	53	24	PALL-2500QAT	C	C		grav.	EUSAAR-2
KOS	Kosetice	49°35′N	15°05′E	534	20	24	PALL-2500QAT	Y	Y	Y	grav.[a]	EUSAAR-2
KPS	*K-puszta*	*46°58′N*	*19°35′E*	*125*	*20*	*24*	*Whatman QMA*	*C*		*C*	*N/A*	TOC[b]
FIK	Finokalia	35°19′N	25°40′E	250	46	24	*Whatman QMA*				β-gauge	EUSAAR-2
MEL	Melpitz	51°32′N	12°56′E	86	53	24	Munktell MK360				grav.	VDI2465[c]
IPR	Ispra	45°48′N	8°38′E	209	20	24	PALL-2500QAT	Y		C	grav.	EUSAAR-2

QbQ = quartz behind quartz; QbT = quartz behind Teflon; Y = used all year roud; C = used for specific campaigns only.
grav. = gravimetry; TEOM = tapered element oscillating microbalance; N/A = not applicable.
[a] Gravimetric analyses of PTFE filters sampled simultaneously.
[b] Total Organic Carbon analyser.
[c] VDI 2465 Part 2 modified as follows: 8 min at 650°C in N_2, followed by 8 min at 650°C in O_2. No charring correction.

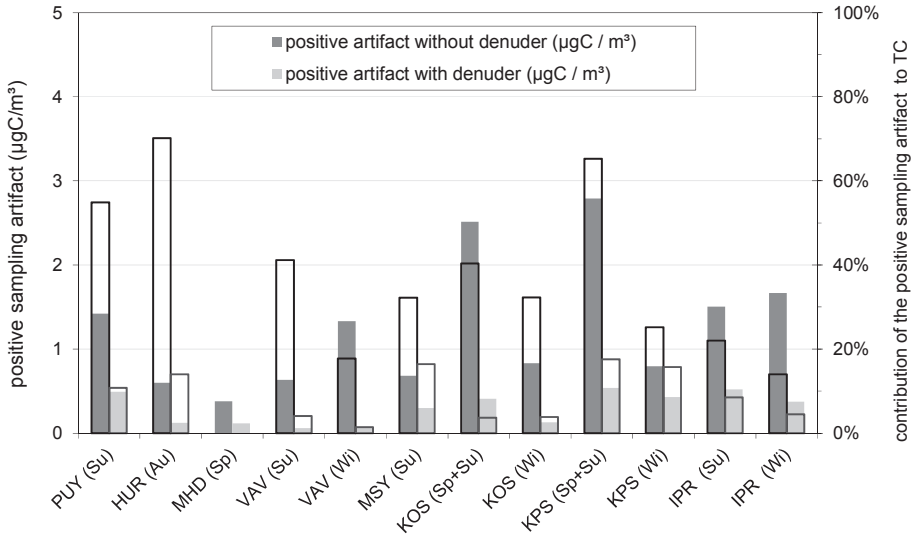

Fig. 2. Seasonal average positive sampling artefacts from bare (left hand side bars) and denuded (right hand side bars) quartz fibre filters observed at 8 regional background sites across Europe. Solid bars show artefacts in µgC/m^3 (left hand scale), and open bars the contribution of artefacts (%) to the amount of TC collected by the quartz fibre filter (right hand scale).

(median = 8%) of the amount of C that would be collected by a bare quartz fibre filter when the EUSAAR denuder is used (Fig. 2). Even if the denuder efficiency is not 100%, such low to marginal sampling artefacts are acceptable, and in any case considerably reduced compared to the artefacts occurring without any denuder. As denuders remove gaseous organic compounds, they could shift the equilibrium of semi-volatile particulate organic compounds (which have significant saturation vapour pressures) towards the gas phase and thus lead to losses in particulate OC. Tests showed no detectable negative artefact induced by the EUSAAR denuder (Fig. S4).

2.2.4. Sampling artefact correction

Carbonaceous aerosol data obtained at APT, VAV, KOS and IPR using the EUSAAR denuder (Fig. S1) were not further corrected for artefacts.

KOS data for Jan. 2009–Aug. 2011 were corrected for positive artefacts according to the QbQ method. For PUY, BIR, MSY, and IPR (for the PM_{10} fraction), OC data were corrected for positive sampling artefacts based on the evaluation of the tests performed at these sites (actually at HUR for BIR) for at least 1 season. Resulting annual mean correction factors for OC range 0.37–0.86 (Table 2). The correction of the positive sampling artefact based on back-up filter data remains quite uncertain (e.g. Subramanian et al., 2004). Using data obtained from specific experiments rather than values measured concomitantly with each PM sampling for particulate carbon measurement further increases this uncertainty, since the representativeness of the data obtained over a limited period of time is unknown. However, the results of these specific tests cannot be ignored. Taking them into account probably improves the accuracy of the data but reduces their precision.

No correction of positive artefacts could be applied to the data obtained at HRL, FIK, and MEL, due to the lack of data regarding sampling artefacts at these sites.

OC data were not corrected for negative artefacts at any site, since relevant data (available from IPR only) suggest that negative artefacts are negligible (see section 2.2.2).

PM gravimetric measurements were corrected for errors due to positive sampling artefacts for OC, but not for additional artefacts, such as losses of NH_4NO_3 during warm periods.

The level of effort directed at addressing sampling artefacts at each site is reflected in the uncertainty assessment (section 2.4, Table 3); uncertainties in positive artefacts are smaller when a denuder is used, and greater where sampling artefacts were determined during campaigns only. An estimated high uncertainty value was used for sites where sampling artefacts were not assessed.

2.3. Analytical discrepancies: assessment and correction

To assess possible differences between laboratories in the determination of TC, OC and EC, inter-laboratory comparison exercises (ILCE) for such measurements, based on ambient PM test samples, have been organized yearly since 2006 as part of the European projects EUSAAR and ACTRIS. All the laboratories which produced data presented here participated in at least one ILCE. Standard deviation discrepancies in TC determination compared to the reference values (defined as the robust averages among all participants) were generally within ±25%, the highest relative discrepancies corresponding to samples with TC loadings < 15 µgC/cm^2 (Fig. 3).

Since no systematic bias in TC determination was observed among the laboratories that produced the data discussed here, no correction of TC values for analytical biases was needed.

Considering that TC, OC, and EC values are not independent from each other, we evaluated possible analytical biases in the determination of the split between OC and EC by examining the EC/TC ratios produced by the participants in the ILCEs.

The systematic differences in determining the EC/TC ratio observed among the various laboratories in the ILCEs performed between 2008 and 2011 (Fig. 4) were used to account for the between-laboratory analytical discrepancies. Thus, correction factors were applied to convert the EC/TC ratios obtained by the various laboratories to values that would have been measured by a virtual reference instrument measuring the same EC/TC ratio as the robust average of all instruments running the EUSAAR-2 protocol. Correction factors for the EC/TC ratios ranged from 0.52 to 1.36 (Table 2).

2.4. Uncertainty estimates

The uncertainties in TC related to sampling artefacts were estimated from the variability (= 1 standard deviation) in the sampling

Table 2
Mean correction factors for OC and EC concentrations.

	Size fraction	Mean OC correction for sampling artefacts	Mean EC correction for analytical bias
PUY	PM10	0.37	0.83
BIR	PM2.5	0.83	0.98
	PM10	0.86	
APT	PM10	NA	0.74
HRL	PM10	ND	0.69
VAV	PM10	NA	1.36
MSY	PM2.5	0.87	1.03
	PM10	0.87	
KOS	PM2.5	NA	1.07
FIK	PM10	ND	0.84
MEL	PM2.5	ND	0.52
	PM10	ND	0.56
IPR	PM2.5	NA	1.05
	PM10	0.76	

NA: not applicable.
ND: not determined.

Table 3
Relative random uncertainties (1 standard deviation) for single measurements. *Italics* denote values estimated from data obtained at other sites.

	TC				EC/TC
	Analytical	Positive artefact	Negative artefact	Combined	Analytical
PUY	13%	17%	5%	22%	37%
BIR	14%	35%	5%	39%	13%
APT	12%	*2%*	5%	*13%*	57%
HRL	12%	*35%*	5%	*38%*	69%
VAV	16%	2%	5%	17%	19%
MSY	26%	20%	5%	33%	23%
KOS	20%	13%	5%	25%	18%
FIK	9%	*35%*	5%	*37%*	31%
MEL	27%	*35%*	5%	*44%*	42%
IPR (PM2.5)	15%	*5%*	5%	17%	18%
IPR (PM10)	15%	10%	5%	19%	18%

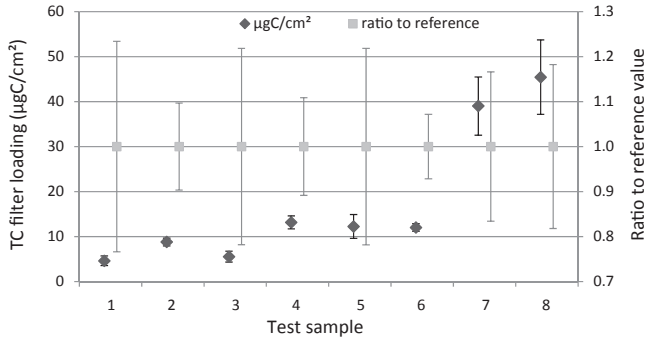

Fig. 3. Range of concentrations and ratios to the reference values for TC concentrations reported for 8 tests samples by the 13 participants in the EUSAAR inter-laboratory comparison of 2008. Error bars show 1 standard deviation.

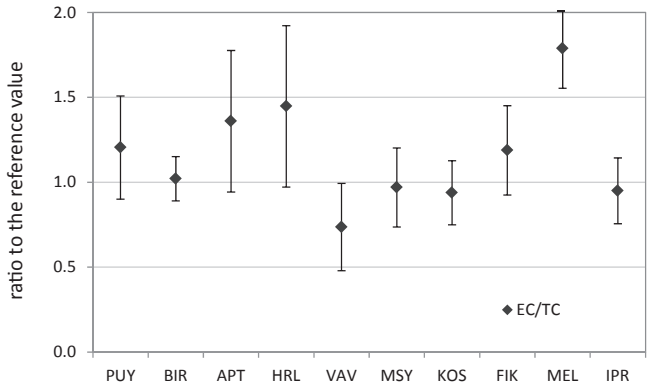

Fig. 4. Average ratio to the reference value of the EC/TC ratio reported by the participants in the inter-laboratory comparisons performed in 2008, 2009 and 2011. Participants are identified by the station which they analyse samples from. The reference value is the robust average among the participants using the EUSAAR-2 analytical protocol. Error bars represent 1 standard deviation.

artefacts observed with the sampling train used for routine measurements at each site. At APT, VAV, KOS (from Sep. 2011) and IPR ($PM_{2.5}$), where a denuder was implemented for routine measurements, the impact of the residual artefacts on the uncertainties in TC is particularly limited (≤5%). For KOS (Feb. 2009–Aug. 2001), the uncertainty of the positive artefact correction based on daily back-up filter measurements (13%) was calculated from the comparison with the results obtained with the EUSAAR sampling train for 15 days. At PUY, BIR, and MSY, ratios between artefact-free TC concentrations and TC concentrations obtained with the routine sampling train were obtained during specific experiments (see supplementary material, section A2). The standard variations of these ratios (17–35%) are used as an estimate of the random error related to the correction of the positive artefacts (Table 3). For HRL, FIK, and MEL, for which no information related to sampling artefacts is available, the maximum uncertainty value observed among all sites (35%) is used. Negative artefacts were studied at IPR only, and their variability observed at this site (±5%) is used as an estimate of the uncertainty related to negative sampling artefacts for all sites.

The analytical uncertainties in TC and EC/TC are estimated as the

variability (1 standard deviation) in the ratios to the reference values observed across the ILCEs organized from 2008 to 2011. These errors combine the repeatability and the reproducibility of the measurements. They range from 9 to 27% and from 13 to 69% for TC and EC/TC, respectively (Table 3). For TC, the analytical, positive artefact and negative artefact uncertainties are assumed to be independent and are added in quadrature to form the combined relative uncertainty.

2.5. Data processing

Obvious erroneous data points (e.g. TC > PM) were discarded. In addition, the data points out of the range [data frequency distribution mode ± two standard deviations] for EC/TC and TC/PM (section 3.3) were considered as outliers and thus discarded too.

Carbonaceous aerosol data from the 10 sites were then made comparable by correcting the OC and TC values for positive sampling artefacts where bare quartz fibre filters were used (2.2), and by correcting the EC values for analytical discrepancies (2.3).

To assess the statistical significance of the differences between averages in carbonaceous aerosol data relative to various sites or different season, Welch's *t*-test for independent samples with unequal variances was apply with a confidence level of 99.9%. Even if the distributions in the various variables are not always normal, the number of data if sufficiently large (n > 120) so that this test can be applied.

3. Results and discussion

3.1. Data coverage

The data sets we discuss cover at least 2 full years between 2008 and 2011 (Fig. 5). This ensures the temporal representativeness of the data sets and limits the impact of inter-annual variability on their comparability. The average concentrations shown in Figs. 6 and 7 are calculated from several hundreds of data collected over at least 2 years. The even distribution of data across these years ensures that these averages are representative for annual averages (no seasonal bias). However, PM_{10} and $PM_{2.5}$ data do not always come from parallel sampling, which means that the temporal coverage for these 2 data sets can be different.

3.2. Annual averages

3.2.1. PM, TC and EC mass concentrations

In Fig. 6, sites are sorted by ascending PM mass concentration values. Note that there are no PM data available from PUY. The lowest concentrations (≤10 μg/m^3) are observed at sites located in North-western Europe, and the highest concentrations (≥20 μg/m^3) in Southern and Central Europe, in line with the observations from Putaud et al., 2010. PM concentrations reflect primary and secondary regional source strengths, the impact of long-range transport of particulate matter, and the dilution of particulate air pollution related to the distance from sources, meteorology and orography.

The corrections for positive sampling artefacts applied to TC data obtained at PUY, BIR, MSY, and IPR (PM_{10} fraction) range from −14 to −33%, and hardly affect the TC concentration gradient from 1 to 9 μgC/m^3 (Fig. 7), which is similar but about twice as pronounced as the gradient in PM mass concentrations. In the case of PUY, the correction for positive artefacts led to the smallest TC concentrations among the 10 sites.

The corrections for analytical biases applied to EC/TC ratios (range 0.52–1.36) perceptibly affect the geographical gradient in EC concentrations (0.1–2 μgC/m^3), which is again about twice as steep as the gradient observed for TC (Fig. 7). These corrections pull EC concentrations in MEL down to values close to those observed in KOS and HRL, and leave IPR alone with an annual average EC concentration well above 1 μgC/m^3 (Table 4).

3.2.2. PM and carbonaceous aerosol composition (TC/PM and EC/TC ratios)

Pollution dilution, related to the distance from sources and to the horizontal and vertical dispersion rate (controlled by meteorology and regional geography), can lead to large differences in atmospheric concentrations of short-lived pollutants such as PM. This can mask similarities and/or differences in the nature of particulate pollution, which can be better described by looking at its composition, e.g. the ratio TC/PM or the contribution of EC to TC in both the PM_{10} and $PM_{2.5}$ size fractions.

Thus, Fig. 8 does not show the geographical gradients observed in Figs. 6 and 7, although TC/PM is significantly higher in IPR, where TC and PM concentrations are highest too. In contrast, the second highest TC/PM ratio is observed at APT in Scandinavia, where PM_{10} mass concentrations are among the lowest, while TC/PM ratios are among the lowest at the Mediterranean sites FIK and MSY, where PM mass concentrations are among the highest. TC/PM ratios in PM_{10} in BIR, HRL and MEL are all between 0.14 (as observed in VAV) and 0.24 (as observed in APT). This shows that PM chemical composition can differ more within a given region (APT and VAV are located a few hundreds of km from each other) than across the whole continent. TC/PM ratios in $PM_{2.5}$ in BIR, MSY, and MEL are also quite similar (range 0.15–0.20). TC/PM ratios are significantly greater in $PM_{2.5}$ compared to PM_{10} at all three sites (BIR, MSY, and IPR) where artefact-corrected data are available for both size fractions. This suggests a larger contribution of non-carbonaceous species (e.g. mineral dust, sea salt) to the coarse aerosol fraction at these sites. The similarity of the Mediterranean sites MSY and FIK regarding TC concentrations (Fig. 7, top) is confirmed by alike TC/PM ratios at those sites.

The regional mean TC/PM ratios calculated from the data obtained at our 10 regional background sites in 2008–2011 (0.25 and 0.19 in $PM_{2.5}$ and PM_{10}, respectively) are compared with ratios calculated from literature data for rural sites in Europe (Putaud et al., 2010), from the IMPROVE (Interagency Monitoring of Protected Visual Environment) sites in the USA (Hand et al., 2011), and from rural sites in China (Wang et al., 2016) and India (Ram and Sarin, 2010, 2012; Bisht et al., 2015). TC/PM regional mean ratios appear quite incredibly similar in all the studies we tabulated, although the number of sites, the levels of PM concentrations, and the handling of sampling artefacts are very different. This can probably not be interpreted as an indication that the mix of sources leading to particulate pollution is similar at all rural sites across the whole world. Further work would be needed to explain this observation.

The range of EC/TC average values corrected for sampling artefacts and analytical biases shown in Fig. 9 (0.10–0.23) is rather narrow compared to any other variable discussed so far. Corrections are especially significant for PUY (due to sampling artefacts) and MEL (due to analytical biases). While non-corrected data would make PUY and MEL the 2 stations with the most extreme EC/TC mean values, corrections bring them back close to the average value among all sites (0.16, Table 4). There is no clear gradient in EC/TC ratios from PUY to IPR, and significant differences in EC/TC mean ratios cannot be detected between BIR, HRL and FIK, PUY and MEL, VAV and MSY in PM_{10}, and between BIR, MSY, KOS and MEL in $PM_{2.5}$. Except for APT on the one hand and IPR on the other hand, all EC/TC ratios sit between 0.13 and 0.18. The EC/TC ratio is not significantly different in $PM_{2.5}$ compared to PM_{10} at three of the sites where data for both fractions are available (MSY, MEL, IPR), but

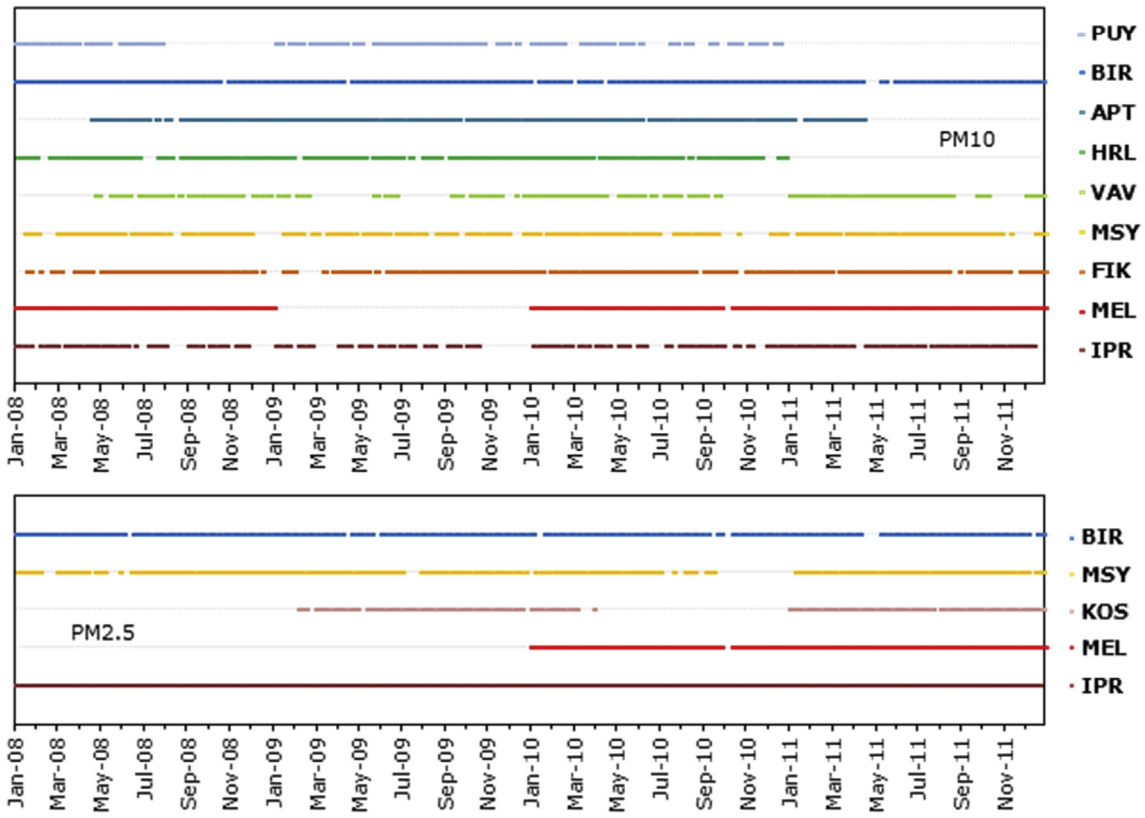

Fig. 5. Temporal coverage for the carbonaceous species data in PM_{10} (top) and $PM_{2.5}$ (bottom).

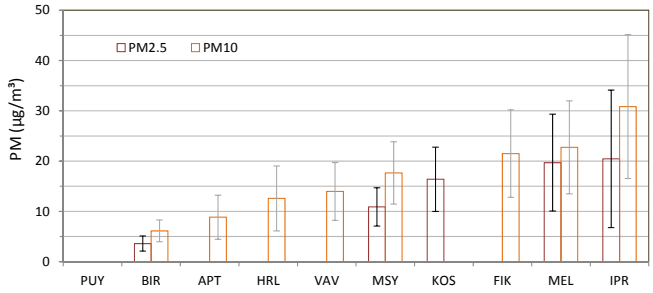

Fig. 6. Average PM_{10} and $PM_{2.5}$ mass concentrations at 10 sites across Europe. No PM mass concentration values are available for PUY. Error bars show one mean absolute deviation around averages.

in BIR, where high levels of primary biological coarse particles occur during a part of the year (Yttri et al., 2011b).

We did not tabulate the EC/TC ratios obtained from other studies for comparison with our results because various analytical methods lead to so different OC/EC splits that this could have been very misleading.

Particulate organic matter (OM) also contains H, O, and other atoms as well as carbon. Assuming a constant OM/OC ratio of 1.4, corresponding to the low limit among the estimates available so far (Turpin and Lim, 2001), we estimated from the mean EC/TC and TC/PM ratios observed at our 10 stations (0.10–0.23, and 0.11–0.42, respectively) that the carbonaceous aerosol accounts for minimum 15–43% of PM_{10} and 21–56% of $PM_{2.5}$ at regional background sites across Europe.

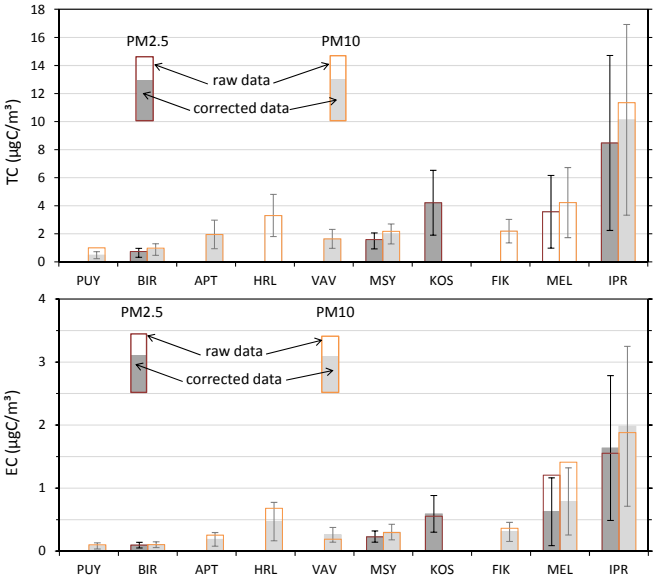

Fig. 7. Average concentrations of TC (top) and EC (bottom) in $PM_{2.5}$ and PM_{10} for the same sites as in Fig. 6. Open bars represent the raw data obtained at the stations, and full bars the concentrations corrected for sampling artefacts and analytical biases (see text). Error bars show one mean absolute deviation around corrected averages.

3.3. *Seasonal frequency distributions and variations in the concentrations of PM and its carbonaceous fractions*

Even at a given site and for a given season, the variability in the TC/PM ratio is large (the relative standard deviation is in the range

Table 4
Average mass, TC, EC concentrations (μg/m^3) and ratios observed at regional (rural) background sites, corrected for sampling artefacts and analytical biases (excepted when in italics) in the $PM_{2.5}$ and PM_{10} size fractions.

	$PM_{2.5}$					PM_{10}					Reference
	Mass	TC	TC/PM	EC	EC/TC	Mass	TC	TC/PM	EC	EC/TC	
PUY							0.5		0.1	0.18	
BIR	3.5	0.7	0.20	0.1	0.16	6.0	0.9	0.16	0.1	0.13	
APT						8.8	2.0	0.24	0.2	0.10	
HRL						12.6	*3.3*	*0.22*	0.5	*0.13*	
VAV						14.0	1.6	0.14	0.3	0.16	
MSY	10.8	1.5	0.15	0.2	0.17	17.5	2.0	0.12	0.3	0.16	
KOS	16.4	4.2	0.31	0.6	0.15						
FIK						21.5	*2.2*	*0.11*	0.3	*0.14*	
MEL	19.7	3.6	0.16	0.6	0.17	22.7	*4.2*	*0.17*	0.8	*0.18*	
IPR	20.5	8.5	0.42	1.6	0.22	29.2	10.1	0.34	2.0	0.22	
Av. Europe			0.25		0.17			0.19		0.16	This work
Av. Europe			*0.19*					*0.20*			Putaud et al., 2010
Av. USA			0.25								Hand et al., 2011
Av. China			*0.22*					*0.21*			Wang et al., 2016
Av. India[a]			*0.20*					*0.22*			Ram and Sarin, 2010, 2012; Bisht et al., 2015

[a] The data from India come from 1 site only for $PM_{2.5}$, and from a combination with Total Suspended Particulate matter (TSP) data for PM_{10}.

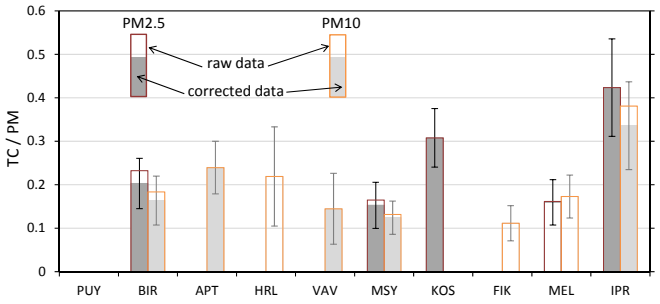

Fig. 8. Average TC/PM ratios in $PM_{2.5}$ and PM_{10}. Open bars represent the raw data obtained at the stations, and full bars the values corrected for sampling artefacts (see text). No PM data are available for PUY. Error bars show one mean absolute deviation around corrected averages.

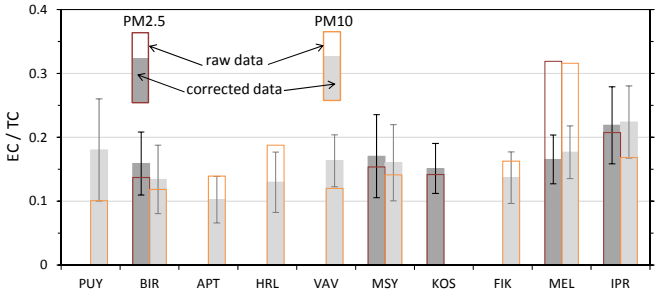

Fig. 9. Average EC/TC ratios in $PM_{2.5}$ and PM_{10} for the same sites as in Fig. 6. Open bars represent the raw data obtained at the stations, and full bars the values corrected for sampling artefacts and analytical biases (see text). Error bars show one mean absolute deviation around corrected averages.

25–65%). However, the frequency distributions of the TC/PM ratio in PM_{10} are mono-modal and generally rather narrow in APT, MSY, MEL and IPR (Fig. 10a). This could indicate that the sources of PM_{10} at these sites do not vary much within each season (and even across the whole year for APT). Clearly bi-modal distributions can be observed at 3 other sites (HRL, VAV, FIK). Four modes can be distinguished in the TC/PM_{10} frequency distribution in BIR, which combine with different weightings across the year, resulting in the fact that TC/PM ratios >0.3 are observed evenly across the year, while ratios <0.1 are also observed in all seasons but summer. Processes which could explain such observations have been discussed by Ricard et al. (2002) and Yttri et al. (2011a). At two of the sites where $PM_{2.5}$ data are also available (MEL and IPR), both the frequency distribution shapes and modes (Fig. 10b) are generally similar to those observed in PM_{10} (although the data coverage is not always the same for both size fractions). This is not the case in BIR and MSY. In BIR the TC/PM frequency distributions in $PM_{2.5}$ are much less variable compared to PM_{10}. The comparison between these 2 size fractions suggests the occurrence of variable non-carbonaceous coarse aerosol (possibly sea salt) from spring to autumn. In contrast, the distributions of the TC/PM ratio frequency at MSY show more variability in $PM_{2.5}$ than in PM_{10}. At KOS (where only $PM_{2.5}$ data are available), the frequency distributions of TC/$PM_{2.5}$ are quite narrow (relative standard deviation < 30%). Ratios <0.2 are more frequent in summer and ratios >0.3 are more frequent in winter.

The variability in the EC/TC ratio for a given season and site (relative standard deviation ranging from 20 to 50%) is generally smaller than the variability in the TC/PM ratio, but the seasonal variations appear larger, except for MEL and IPR (Fig. 11a). In PM_{10}, the variability in the contribution of EC to TC increases with decreasing levels of particulate pollution: at PUY (the least polluted site) in summer, EC/TC ratios <0.05 or >0.50 are frequently observed, while in MEL and IPR (the two most polluted sites), such extreme ratios seldom occur. The most frequent EC/TC ratios observed at MEL and IPR (0.15–0.20) are also very common at all other sites, especially in winter. The frequency distributions of EC/TC in $PM_{2.5}$ are very similar to those observed in PM_{10} for MEL and IPR (Fig. 11b). In BIR, noticeable differences are observed from spring to autumn, where the lowest EC/TC ratios occurring in PM_{10} are not observed in $PM_{2.5}$. Such seasonal variations suggest again a specific contribution of primary biogenic OC to the coarse aerosol fraction of PM10, which has previously been demonstrated by Yttri et al. (2007b, 2011a).

Monthly averages calculated over several years are shown in Fig. 12. The seasonal variations in PM mass concentrations (Fig. 12a) are different in shape and magnitude across the sites of the network. Winter time maxima and summer time minima can be observed at various locations including continental sites (IPR, MEL, KOS), southern Scandinavia (VAV), and Great Britain (HRL), while an opposite cycle (maximum in summer) is observed at the Mediterranean site MSY. No clear seasonal cycle in PM_{10} mass concentration is observed at other sites (FIK, APT, BIR). Similar seasonal variations are generally observed in both PM_{10} and $PM_{2.5}$ fractions.

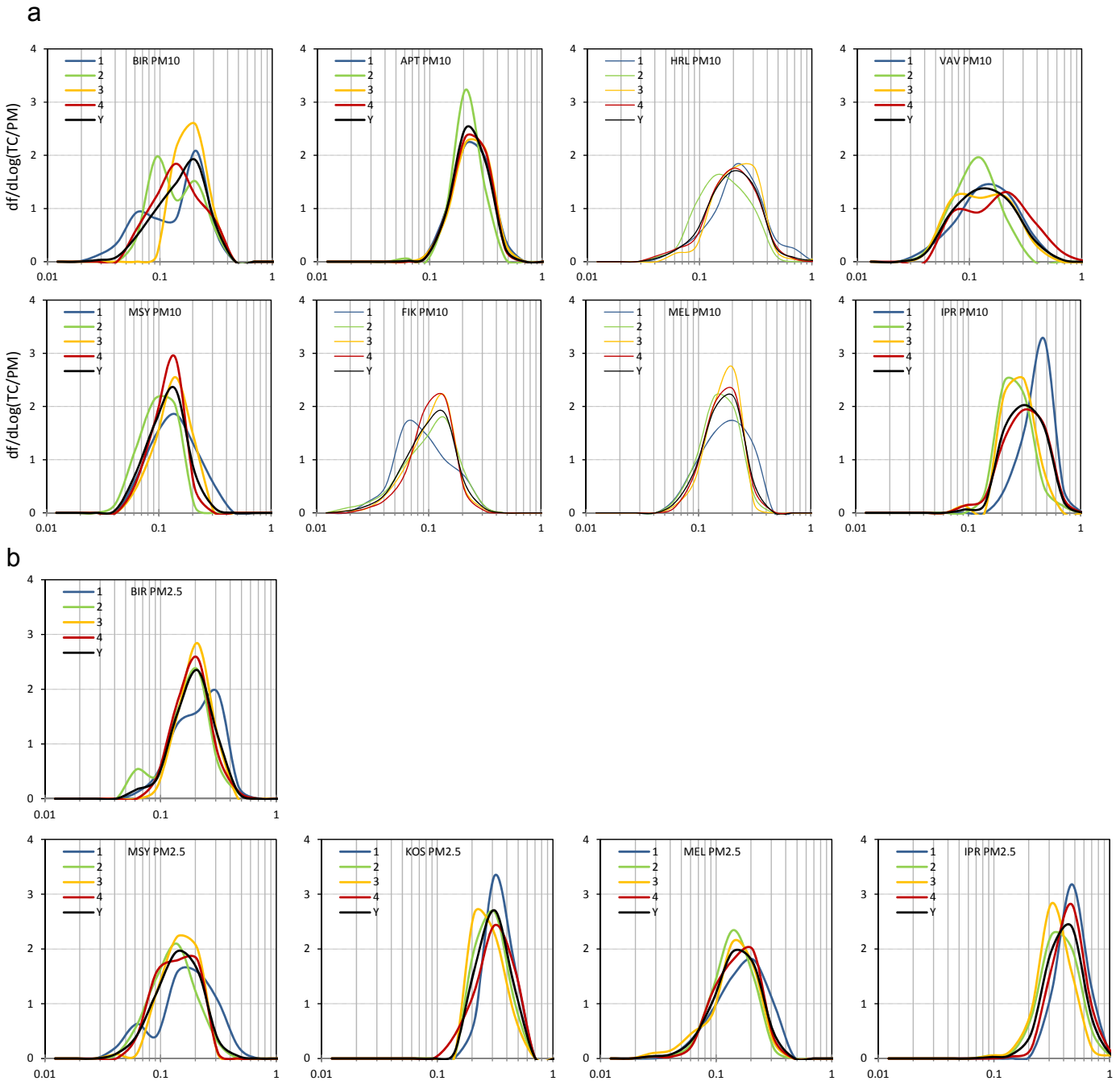

Fig. 10. a: seasonal and annual (Y) mean frequency distribution of the ratio TC/PM10 (1 = DJF, 2 = MAM, 3 = JJA, 4 = SON). Thin lines represent distributions at sites where positive sampling artefacts were not addressed. b: The same as 10a for the PM2.5 size fraction.

An exception is BIR again, where clearer seasonal variations are observed in $PM_{2.5}$ (maximum in spring) compared to PM_{10}.

Similar seasonal variations are also observed for the carbonaceous fractions TC, OC, and EC. We will therefore focus our discussion on the TC/PM and EC/TC ratios.

Fig. 12b shows monthly mean TC/PM ratios ranging between about 0.1 and 0.5 across the various sites. TC/PM monthly averages can be quite variable at some sites (relative standard deviation up to 24%). The seasonal variations are more pronounced in PM_{10} than in $PM_{2.5}$ at most sites, which highlights the weight of coarse particles in PM_{10} at those sites. A clear (smooth) seasonal cycle can be observed at a few sites only, including IPR and APT. At IPR, the seasonal cycle of TC/PM is characterized by high values in November, December, and January, and lower values between May and August. A similar cycle can be observed in MSY for both size fractions, although secondary maxima can also be observed in summer, every year between 2008 and 2011 (data not shown). In KOS, the greatest TC/PM ratios are also observed in November and December. Such seasonal cycles can be explained by an increase in carbonaceous aerosol emission due to domestic heating during cold months (Gilardoni et al., 2011; Schwarz et al., 2016). In contrast, the seasonal cycle in APT shows a maximum in August and a minimum in spring. Larger TC/PM values are also observed in BIR from May to September in PM_{10} (as already suggested from the

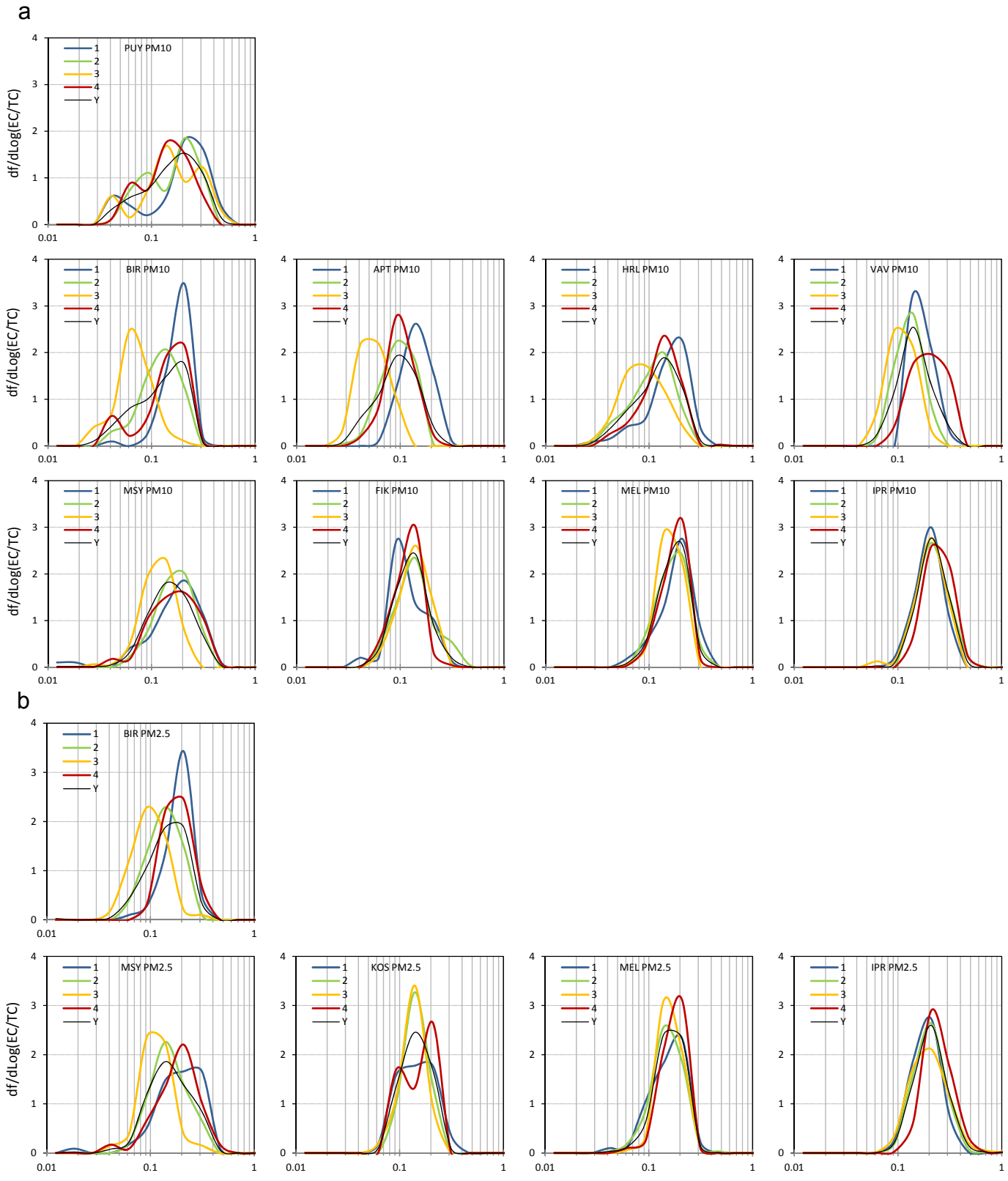

Fig. 11. a: same as Fig. 10a for the EC/TC ratio. b: The same as 11a for the PM2.5 size fraction.

frequency distributions). At these sites, stronger sources of coarse primary biogenic aerosols during warmer months could explain these observations (Yttri et al., 2011b). Large inter-annual variations make it difficult to highlight robust seasonal cycles at the other sites, suggesting that seasonal variations in various sources of carbonaceous aerosol can compensate each other (Charron et al.,

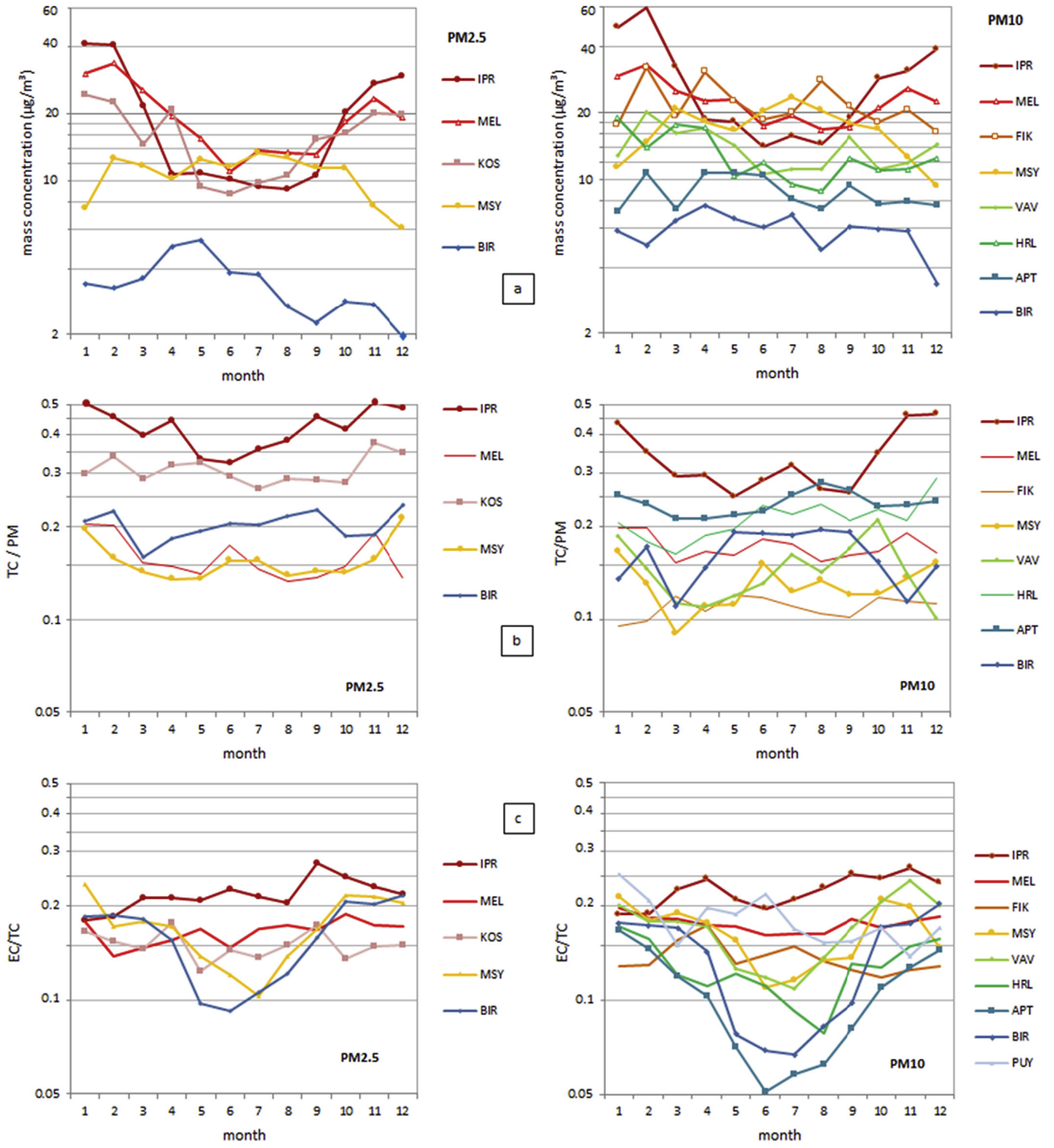

Fig. 12. Seasonal variations in (a) PM mass concentrations, (b) TC/PM and (c) EC/TC ratios. Lines without full symbols correspond to the sites for which sampling artefacts were not addressed (see text).

2013; Genberg et al., 2013; Minguillón et al., 2015; Bougiatioti et al., 2013; Spindler et al., 2013).

EC/TC monthly mean ratios range from 0.05 to 0.4 across the various sites and the 12 months of the year (Fig. 12c). Interestingly, the spatial gradient in EC/TC follows quite well the spatial gradient in PM mass concentration (Fig. 12a) for summer months, whereas EC/TC ratios are much more similar at all sites during winter (e.g. 0.18–0.25 in January, excluding FIK, 0.13). An exception is the mountain top site PUY, where summertime EC/TC ratios are not as low as at sites with similarly low aerosol concentrations. This might be due to upslope winds which bring to PUY air from the nearby urban and industrial areas in summer during daytime (Freney et al., 2011). The seasonal variations in the EC/TC ratio at IPR, MEL, FIK and KOS are small (relative standard deviation 6%–14%). This could be

explained by the predominance of a single source of carbonaceous aerosol at these sites, or by different sources of OC occurring in winter (e.g. wood burning for domestic heating) and summer (e.g. secondary organic aerosol formation) which compensate each other. For all other sites, there is a pronounced seasonal cycle in EC/TC with a clear minimum during summer. This minimum is more marked at more remote sites, as well as in the PM_{10} fraction compared to the $PM_{2.5}$ fraction. These observations suggest a significant contribution of biogenic sources to the PM mass concentration in BIR, APT, VAV (Scandinavia), HRL (Great Britain), and MSY (Western Mediterranean basin).

4. Conclusions

Commercial carbon monolith denuders efficiently mitigate the sampling artefacts that can affect the determination of particulate organic carbon. At the sites where denuders were not used, positive sampling artefacts contributed between by 14 and 70% (site average) to the amount of TC collected by bare quartz fibre filters at regional background sites across Europe. The data we obtained on sampling positive artefacts allowed us to correct the OC data collected from most sites where a denuder was not routinely applied.

Yearly comparisons between the analysers used across the network showed that no recurrent biases in TC determination could be detected. In contrast, systematic differences in the OC/EC split determined by the various instruments were observed. They were taken into account to normalize the data provided by different laboratories.

The consistency between the carbonaceous aerosol measurements performed across the network would be enhanced by the implementation of the denuder (at least for low volume samplers), the application of the future European standard (EN16909) for the analyses, and the use of suitable certified reference materials.

Unlike our previous "phenomenologies" (Putaud et al., 2004, 2010; Van Dingenen et al., 2004), this work arose from a coordinated action at the European scale aiming at producing comparable TC, OC and EC data. As a consequence, it emphasises the production of more robust data with better known uncertainties. It confirms that the atmospheric concentrations of PM_{10} and $PM_{2.5}$ carbonaceous constituents (TC, OC and EC) increase when moving from Scandinavia to Central Europe through the Mediterranean area. The spatial gradients in the PM carbonaceous content (TC/PM ratio) and the composition of this carbonaceous fraction (EC/TC ratio) are much less pronounced than the gradient in concentrations, which mainly reflects the atmospheric pollution dilution. Carbonaceous species account for a significant fraction of PM_{10} (15–43%) and even more so of $PM_{2.5}$ (21–56%). At several sites, the TC/PM ratio is highest during winter months, when exceedances of particulate pollution daily limits usually occur. EC/TC ratios are also high and quite similar (0.13–0.25) at all the sites of the network during the cold months, which suggests that the dominant sources of carbonaceous aerosol are the same at all sites in winter.

This survey provides a robust assessment of the carbonaceous aerosol concentrations, composition, and contribution to PM_{10} and $PM_{2.5}$ at the time where European member states had to start measuring the chemical composition of $PM_{2.5}$ (including OC and EC) at rural sites, according to the European Directive 2008/50/EC.

Acknowledgements

EUSAAR (FP6/2001-2006, grant agreement no. RII3-GT-2006-026140), ACTRIS (FP7/2007-2013, grant agreement no. 262254), ACTRIS2 (H2020-INFRAIA-2014-2015, grant agreement no. 654109), EPA Ireland is acknowledged for the research support at Mace Head, the Norwegian Environment Agency for the measurements at Birkenes.

Appendix A. Supplementary data

Supplementary data related to this article can be found at http://dx.doi.org/10.1016/j.atmosenv.2016.07.050.

References

Baumgardner, D., Popovicheva, O., Allan, J., Bernardoni, V., Cao, J., Cavalli, F., Cozic, J., Diapouli, E., Eleftheriadis, K., Genberg, P.J., Gonzalez, C., Gysel, M., John, A., Kirchstetter, T.W., Kuhlbusch, T.A.J., Laborde, M., Lack, D., Müller, T., Niessner, R., Petzold, A., Piazzalunga, A., Putaud, J.P., Schwarz, J., Sheridan, P., Subramanian, R., Swietlicki, E., Valli, G., Vecchi, R., Viana, M., 2012. Soot reference materials for instrument calibration and intercomparisons: a workshop summary with recommendations. Atmos. Meas. Tech. 5, 1869–1887.

Birch, M.E., Cary, R.A., 1996. Elemental carbon-based method for monitoring occupational exposures to particulate diesel exhaust. Aerosol Sci. Technol. 25, 221–241.

Bisht, D.S., Srivastava, A.K., Pipal, A.S., Srivastava, M.K., Pandey, A.K., Tiwari, S., Pandithurai, G., 2015. Aerosol characteristics at a rural station in southern peninsular India during CAIPEEX-IGOC: physical and chemical properties. Environ. Sci. Pollut. Res. 22, 5293–5304.

Boucher, O., Randall, D., Artaxo, P., Bretherton, C., Feingold, G., Forster, P., Kerminen, V.-M., Kondo, Y., Liao, H., Lohmann, U., Rasch, P., Satheesh, S.K., Sherwood, S., Stevens, B., Zhang, X.Y., 2013. Clouds and aerosols. In: Stocker, T.F., Qin, D., Plattner, G.-K., Tignor, M., Allen, S.K., Boschung, J., Nauels, A., Xia, Y., Bex, V., Midgley, P.M. (Eds.), Climate Change 2013: The Physical Science Basis. Contribution of Working Group I to the Fifth Assessment Report of the Intergovernmental Panel on Climate Change. Cambridge University Press, Cambridge, United Kingdom and New York, NY, USA.

Bougiatioti, A., Zarmpas, P., Koulouri, E., Antoniou, M., Theodosi, C., Kouvarakis, G., Saarikoski, S., Mäkelä, T., Hillamo, R., Mihalopoulos, N., 2013. Organic, elemental and water-soluble organic carbon in size segregated aerosols, in the marine boundary layer of the Eastern Mediterranean. Atmos. Environ. 64, 251–262.

Cassee, F.R., Héroux, M.E., Gerlofs-Nijland, M.E., Kelly, F.J., 2013. Particulate matter beyond mass: recent health evidence on the role of fractions, chemical constituents and sources of emission. Inhal. Toxicol. 25 (14), 802–812.

Cavalli, F., Viana, M., Yttri, K.E., Genberg, J., Putaud, J.-P., 2010. Toward a standardized thermal-optical protocol for measuring atmospheric organic and elemental carbon: the EUSAAR Protocol. Atmos. Meas. Tech. 3, 79–89.

Charron, A., Degrendele, C., Laongsri, B., Harrison, R.M., 2013. Receptor modelling of secondary and carbonaceous particulate matter at a Southern UK Site. Atmos. Chem. Phys. 13, 1879–1894.

Chow, J.C., Watson, J.G., Pritchett, L.C., Pierson, W.R., Frazier, C.A., Purcell, R.G., 1993. The DRI thermal/optical reflectance carbon analysis system: description, evaluation and applications in U.S. Air Quality studies. Atmos. Environ. 27A, 1185–1201.

Freney, E.J., Sellegri, K., Canonaco, F., Boulon, J., Hervo1, M., Weigel, R., Pichon, J.M., Colomb, A., Prevot, A.S.H., Laj, P., 2011. Seasonal variations in aerosol particle composition at the puy-de-Dome research station in France. Atmos. Chem. Phys. 11, 13047–13059.

Gilardoni, S., Vignati, E., Cavalli, F., Putaud, J.P., Larsen, B.R., Karl, M., Stenström, K., Genberg, J., Henne, S., Dentener, F., 2011. Better constraints on sources of carbonaceous aerosols using a combined 14C – macro tracer analysis in a European rural background site. Atmos. Chem. Phys. 11, 5685–5700.

Genberg, J., Denier van der Gon, H.A.C., Simpson, D., Swietlicki, E., Areskoug, H., Beddows, D., Ceburnis, D., Fiebig, M., Hansson, H.C., Harrison, R.M., Jennings, S.G., Saarikoski, S., Spindler, G., Visschedijk, A.J.H., Wiedensohler, A., Yttri, K.E., Bergström, R., 2013. Light-absorbing carbon in Europe – measurement and modelling, with a focus on residential wood combustion emissions. Atmos. Chem. Phys. 13, 8719–8738.

Hand, J. L., Copeland, S. A., Day, D. E., Dillner, A. M., Idresand, H., Malm, W. C., McDade, C. E., Moore, Jr., C. T., Pitchford, M. L., Schichtel, B. A., and Watson, J. G.: IMPROVE (Interagency Monitoring of Protected Visual Environments): Spatial and seasonal patterns and temporal variability of haze and its constituents in the United States: Report V, CIRA Report ISSN: 0737-5352-87, http://vista.cira.colostate.edu/improve/Publications/Reports/2011/2011.htm, 2011.

Karanasiou, A., Minguillón, M.C., Viana, M., Alastuey, A., Putaud, J.-P., Maenhaut, W., Panteliadis, P., Močnik, G., Favez, O., Kuhlbusch, T.A.J., 2015. Thermal-optical analysis for the measurement of elemental carbon (EC) and organic carbon (OC) in ambient air a literature review. Atmos. Meas. Tech. Discuss. 8, 9649–9712.

Mader, B.T., Flagan, R.C., Seinfeld, J.H., 2001. Sampling atmospheric carbonaceous aerosols using a particle trap impactor/denuder sampler. Environ. Sci. Technol. 35, 4857–4867.

Minguillón, M.C., Ripoll, A., Pérez, N., Prévôt, A.S.H., Canonaco, F., Querol, X., Alastuey, A., 2015. Chemical characterization of submicron regional background aerosols in the western Mediterranean using an Aerosol Chemical Speciation Monitor. Atmos. Chem. Phys. 15, 6379–6391.

McDow, S.R., Huntzicker, J.J., 1990. Vapor adsorption artifact in the sampling of organic aerosol: face velocity effects. Atmos. Environ. 24, 2563–2571.

Pio, C.A., Legrand, M., Oliveira, T., Afonso, J., Santos, C., Caseiro, A., Fialho, P., Barata, F., Puxbaum, H., Sanchez-Ochoa, A., Kasper-Giebl, A., Gelencsér, A., Preunkert, S., Schock, M., 2007. Climatology of aerosol composition (organic versus inorganic) at non-urban sites on a west-east transect across Europe. J. Geophys. Res. 112, D23S02. http://dx.doi.org/10.1029/2006JD008038.

Putaud, J.P., Raes, F., Van Dingenen, R., Brüggemann, E., Facchini, M.C., Decesari, S., Fuzzi, S., Gehrig, R., Hüglin, C., Laj, P., Lorbeer, G., Maenhaut, W., Mihalopoulos, N., Müller, K., Querol, X., Rodriguez, S., Schneider, J., Spindler, G., Ten Brink, H., Tørseth, K., Alfred Wiedensohler, A., 2004. European aerosol phenomenology — 2: chemical characteristics of particulate matter at kerbside, urban, rural and background sites in Europe. Atmos. Environ. 38, 2579–2595.

Putaud, J.P., Van Dingenen, R., Alastuey, A., Bauer, H., Birmili, W., Cyrys, J., Flentje, H., Fuzzi, S., Gehrig, R., Hansson, H.C., Harrison, R.M., Hermann, H., Hitzenberger, R., Hüglin, C., Jones, A.M., Kasper-Giebl, A., Kiss, G., Kousa, A., Kuhlbusch, T.A.J., Löschau, G., Maenhaut, W., Molnar, A., Moreno, T., Pekkanen, J., Perrino, C., Pitz, M., Puxbaum, H., Querol, X., Rodriguez, S., Salma, I., Schwarz, J., Smolik, J., Schneider, J., Spindler, G., ten Brink, H., Tursic, J., Viana, M., Wiedensohler, A., Raes, F., 2010. A European aerosol phenomenology — 3: physical and chemical characteristics of particulate matter from 60 rural, urban, and kerbside sites across Europe. Atmos. Environ. 44, 1308–1320.

Querol, X., Alastuey, A., Viana, M., Moreno, T., Reche, C., Minguillón, M.C., Ripoll, A., Pandolfi, M., Amato, F., Karanasiou, A., Pérez, N., Pey, J., Cusack, M., Vázquez, R., Plana, F., Dall'Osto, M., De La Rosa, J., Sánchez De La Campa, A., Fernández-Camacho, R., Rodríguez, S., Pio, C., Alados-Arboledas, L., Titos, G., Artíñano, B., Salvador, P., García Dos Santos, S., Fernández Patier, R., 2013. Variability of carbonaceous aerosols in remote, rural, urban and industrial environments in Spain: implications for air quality policy. Atmos. Chem. Phys. 13, 6185–6206.

Ram, K., Sarin, M.M., 2010. Spatio-temporal variability in atmospheric abundances of EC, OC and WSOC over northern India. J. Aerosol Sci. 41 (1), 88–98.

Ram, K., Sarin, M.M., 2012. Carbonaceous aerosols over northern India: sources and spatio-temporal variability. Proc. Indian natl. Sci. Acad. 78, 523–533.

Ricard, V., Jaffrezo, J.-L., Kerminen, V.-M., Hillamo, R.E., Sillanpaa, M., Ruellan, S., Liousse, C., Cachier, H., 2002. Two years of continuous aerosol measurements in northern Finland. J. Geophys. Res. D 107. ACH 10-1–ACH 10-17.

Schwarz, J., Chi, X., Maenhaut, W., Civiš, M., Hovorka, J., Smolík, J., 2008. Elemental and organic carbon in atmospheric aerosols at downtown and suburban sites in Prague. Atmos. Res. 90, 287–302.

Schwarz, J., Cusack, M., Karban, J., Chalupnícková, E., Havránek, V., Smolík, J., Zdímal, V., 2016. $PM_{2.5}$ chemical composition at a rural background site in central Europe, including correlation and air mass back trajectory analysis. Atmos. Res. 176–177, 108–120.

Spindler, G., Grüner, A., Müller, K., Schlimper, S., Herrmann, H., 2013. Long-term size-segregated particle (PM10; PM2.5, PM1) characterization study at Melpitz - influence of air mass inflow, weather condition and season. J. Atmos. Chem. 70, 165–195.

Subramanian, R., Khlystov, A.Y., Cabada, J.C., Robinson, A.L., 2004. Positive and negative artefacts in particulate organic carbon measurement with denuded and undenuded sampler configurations. Aerosol Sci. Technol. 38 (S1), 27–48.

Turpin, B.J., Huntzicker, J.J., 1994. Investigation of organic aerosol sampling artifacts in the Los Angeles basin. Atmos. Environ. 28, 3061–3071.

Turpin, B.J., Lim, H.-J., 2001. Species contributions to $PM_{2.5}$ mass concentrations: revisiting common assumptions for estimating organic mass. Aerosol Sci. Technol. 35, 602–610.

Tørseth, K., Aas, W., Breivik, K., Fjæraa, A.M., Fiebig, M., Hjellbrekke, A.G., Lund Myhre, C., Solberg, S., Yttri, K.E., 2012. Introduction to the European monitoring and evaluation programme (EMEP) and observed atmospheric composition change during 1972–2009. Atmos. Chem. Phys. 12, 5447–5481.

Van Dingenen, R., Putaud, J.P., Raes, F., Baltensperger, U., Charron, A., Facchini, M.C., Decesari, S., Fuzzi, S., Gehrig, R., Hansson, H.C., Harrison, R.M., Hüglin, C., Jones, A.M., Laj, P., Lorbeer, G., Maenhaut, W., Palgren, F., Querol, X., Rodriguez, S., Schneider, J., Ten Brink, H., Tunved, P., Tørseth, K., Wehner, B., Weingartner, E., Wiedensohler, A., Wåhlin, P., 2004. A European aerosol phenomenology–1: physical characteristics of particulate matter at kerbside, urban, rural and background sites in Europe. Atmos. Environ. 38, 2561–2577.

Viana, M., Chi, X., Maenhaut, W., Cafmeyer, J., Querol, X., Alastuey, A., Mikuška, P., Večeřa, Z., 2006. Influence of sampling artefacts on measured PM, OC, and EC levels in carbonaceous aerosols in an urban area. Aerosol Sci. Technol. 40, 107–117.

Wang, L.P., Zhou, X.H., Ma, Y.J., Cao, Z.Y., Wu, R.D., Wang, W.X., 2016. Carbonaceous aerosols over China – review of observations, emissions and climate forcing. Environ. Sci. Pollut. Res. 23, 1671–1680.

Watson, J.G., Chow, J.C., Wa, L., 2005. Summary of organic and elemental carbon/black carbon analysis methods and intercomparisons. Aerosol Air Qual. Res. 5, 65–102.

Watson, J.G., Chow, J.C., Chen, L.-W.A., Frank, N.H., 2009. Methods to assess carbonaceous aerosol sampling artefacts for IMPROVE and other long-term networks. J. Air & Waste Manage. Assoc. 59, 898–911.

WHO Regional Office for Europe, 2013. Review of Evidence on Health Aspects of Air Pollution (REVIHAAP) (Technical report. Copenhagen).

Yttri, K.E., Aas, W., Bjerke, A., Cape, J.N., Cavalli, F., Ceburnis, D., Dye, C., Emblico, L., Facchini, M.C., Forster, C., Hanssen, J.E., Hansson, H.C., Jennings, S.G., Maenhaut, W., Putaud, J.P., Tørseth, K., 2007a. Elemental and organic carbon in PM10: a one year measurement campaign within the European Monitoring and Evaluation Programme EMEP. Atmos. Chem. Phys. 7, 5711–5725.

Yttri, K.E., Dye, C., Kiss, G., 2007b. Ambient aerosol concentrations of sugars and sugar-alcohols at four different sites in Norway. Atmos. Chem. Phys. 7, 4267–4279.

Yttri, K.E., Simpson, D., Stenström, K., Puxbaum, H., Svendby, T., 2011a. Source apportionment of the carbonaceous aerosol in Norway quantitative estimates based on ^{14}C, thermal-optical and organic tracer analysis. Atmos. Chem. Phys. 11, 9375–9394.

Yttri, K.E., Simpson, D., Nøjgaard, J.K., Kristensen, K., Genberg, J., Stenström, K., Swietlicki, E., Hillamo, R., Aurela, M., Bauer, H., Offenberg, J.H., Jaoui, M., Dye, C., Eckhardt, S., Burkhart, J.F., Stohl, A., Glasius, M., 2011b. Source apportionment of the summer time carbonaceous aerosol at Nordic rural background sites. Atmos. Chem. Phys. 11, 13339–13357.